

Analysis of magnetic flux density for airgap eccentricity and bearing faults

Ilker Ozelgin

Abstract—This paper involves current signal frequency analysis for airgap eccentricity and bearing damage in induction motors. Magnetic flux density in the airgap is calculated to get effect of faults on current signal. Equation of characteristic frequencies for eccentricity is revised. In addition, a sudden eccentricity is simulated in short intervals to get effect of bearing damages. Therefore, new frequencies are detected for bearing faults that is related with eccentricity. This knowledge impresses most of the experimental condition monitoring systems and diagnosis systems.

Keywords—Airgap Eccentricity, Bearing Damage, Fault Detection, Induction Motor.

I. INTRODUCTION

Induction motors take important place in factories. Failure of electrical machines causes loss of money so increment of

motor reliability has been studied. The main reason of failures in induction motors are faults such as,

1. Unbalanced rotor
2. Eccentricity
3. Bearing damage
4. Broken bar
5. Winding faults
6. Looseness
7. Oil effect.

These faults can be detected by online monitoring of vibration and current signals to increase the reliability of machines. A review of fault detection is given in [1]-[3]. The main reasons of faults can be arranged as follow,

1. Over temperature
2. Unbalanced temperature

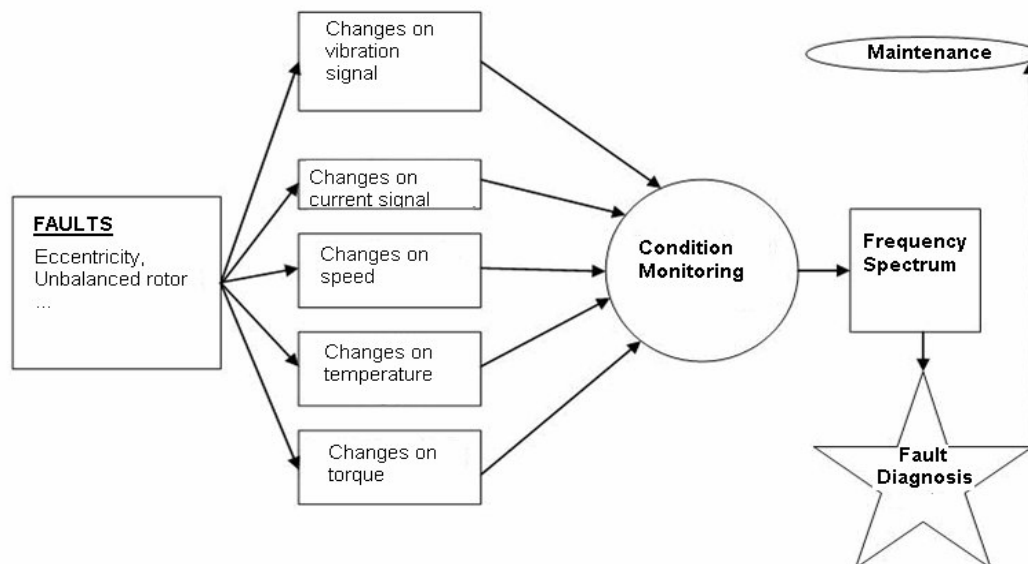


Fig. 1 fault detection

Manuscript received December 13, 2008; Revised version received (), 2009.

The Author is R&D engineer in Ford-Otosan, Kocaeli, Turkey. Phone: +90-262 3156764; fax: +90-262 3156004; e-mail: ozelgin@yahoo.com, iozelgin@ford.com.tr; web page: <http://ozelgin.googlepages.com>.

3. Unbalanced pull-force
4. Electromagnetic force
5. Improper lubrication of bearings

6. Weak shaft and bearing
7. Over speed and load
8. Improper and weak assembling of rotor and stator.

Experimental setups or condition monitoring systems have been established for fault detection of induction machines. Current, vibration, noise, speed, temperature, and torque signals can be used to detect faults in Fig. 1. Generally, current signature analysis has been preferred as [4]-[8]. After data collection, a diagnostic method is necessary to recognize the fault. Different methods have been used to analyze the data e.g. fast fourier transform, wavelet transform, fuzzy logic, neural networks, hilbert transform and new developed methods as in [8]. Recently, software tools have been developed to satisfy the requirements of fault diagnosis and repair of electric machines as in [9]. All experimental studies need correct technical references or reviews to get best result in fault diagnosis. Especially, software based decision systems tend to make wrong decisions.

Reference [1] shows that eccentricity and bearing damage related faults constitute the huge amount of faults. A theoretical method is verified by Thomson [10] to observe eccentricity related frequencies in current and vibration signal. Results of the method are summarized by Vas [11]. Both of the studies have a small wrong at the last formula that calculates eccentricity related frequencies in current signal. Eccentricity is again researched by Guldemir [12].

In this study, magnetic flux density is analyzed for eccentricity related frequencies in current signal. To calculate magnetic flux density, magnetic motor force, and permeance of air-gap are taken into account.

Bearing damage related frequencies in vibration signal are evaluated by kinematical equations. Eccentricity is created instantly in computer program to get effect of bearing damage on current signal. Study of Schoen is confirmed. Also, additional frequencies are expressed.

II. AIRGAP ECCENTRICITY

Nonuniform air-gap is called eccentricity in motors. The main reasons of eccentricity are bad manufacturing tolerances, unbalanced rotor shaft and weak bearing. Eccentricity causes unbalanced magnetic pull, vibration and harmonics in current signal. Eccentricity may be classified in two groups, static eccentricity and dynamic eccentricity.

A. Static Eccentricity

If rotor rotation center is removed a faraway place which is parallel to stator center in Fig. 2. This situation is called static eccentricity. Position of minimum air-gap can not rotate. A magnetic pull force occurs to the side of minimum air-gap. An example for static eccentricity is oval stator as in Fig. 3.

B. Dynamic Eccentricity

Rotor rotates around stator center, but it do not rotate around its center. Hence, minimum airgap and magnetic pull force rotate with rotor. An example for dynamic eccentricity is

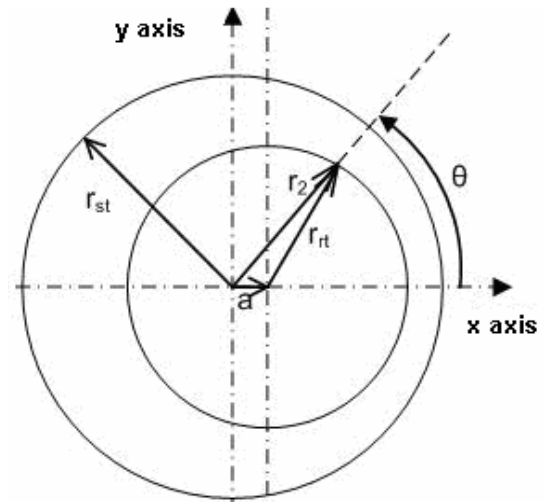


Fig. 2 static eccentricity

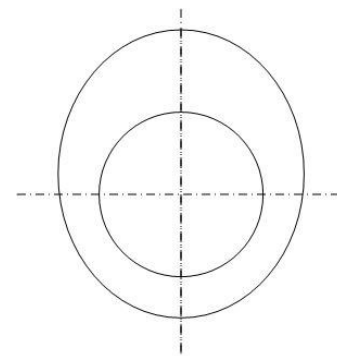


Fig. 3 oval stator

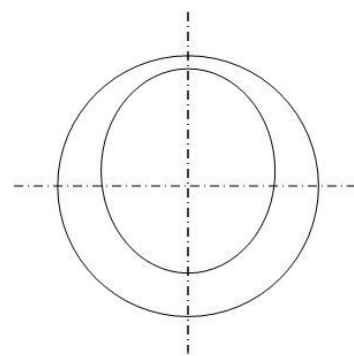


Fig. 4 oval rotor

oval rotor as in Fig. 4.

C. Magnetic Flux Density

Magnetic flux density variation at one point of airgap, which is shown in Fig. 5, gives information about current variation at the nearest coil. This means magnetic flux density calculation at one point behaves as a current sensor.

In reference [13], ampere's circuital law proves the relation between current and magnetic flux density.

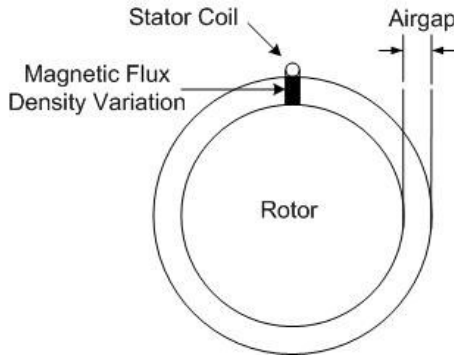


Fig. 5 flux density effect on stator coil

$$\oint B \cdot dx = \mu \cdot I \quad (1)$$

x is any closed path around coil. Formula can be applied for an coil. Current can be calculated as the formula

$$I \approx \frac{\pi \cdot \delta \cdot B}{\mu} \quad (2)$$

δ is length of airgap, μ is permeability of air. Therefore, Magnetic flux density variation is proportional to current signal variation.

Characteristic frequencies of eccentricity on current signal are indicated by calculation of magnetic flux density. Magnetic flux density is the amount of magnetic flux (Φ) per unit area of a section, perpendicular to the direction of flux. Equation (3) is the mathematical representation of magnetic flux density.

$$B = \frac{\Phi}{A} \quad (3)$$

Magnetic flux is related with magnetic motor force (mmf), and reluctance (R) of the magnetic flux path.

$$\Phi = \frac{\text{mmf}}{R} \quad (4)$$

For induction motors, reluctance is the function of airgap length.

$$R = \frac{\delta}{\mu \cdot A} \quad (5)$$

Formula of magnetic flux density can be arranged by using (3)-(5).

$$B = \frac{\text{mmf} \cdot \mu}{\delta} \quad (6)$$

$$B = \mu \cdot \text{mmf} \cdot \lambda \quad (7)$$

λ is permeance. Permeance is the function of airgap length. Permeability of air gap is worse than permeabilities of stator and rotor core. Permeabilities of stator and rotor core are taken infinite. Only, airgap permeability is used. mmf is constructed by stator and rotor mmf. In references [14] and [15], stator and rotor mmf are calculated as following equations.

$$\text{mmf}_{st} = \frac{3\sqrt{2} \cdot N \cdot I_{st}}{\pi \cdot p} \sum_{c_1=0}^{\infty} \frac{1}{\nu} \cdot K_{\nu} \cdot \sin(\nu \cdot \theta \pm w \cdot t) \quad (8)$$

$$\text{mmf}_{rt} = \frac{\sqrt{2} \cdot Z_{rt} \cdot I_{rt}}{\pi \cdot p} \quad (9)$$

$$\sum_{c_2=0}^{\infty} \frac{1}{\xi} \cdot K_{\xi} \cdot \sin(\xi \cdot \theta + (w \cdot \nu \cdot w_r + \xi \cdot w_r) \cdot t)$$

where

- N number of turns at each phase;
- I_{st} stator current;
- p number of pole pairs;
- ν degree of stator harmonics;
- K_{ν} coil factor;
- θ mechanical angle of rotor position;
- w angular supply frequency;
- t time;
- Z_{rt} number of rotor slot;
- I_{rt} rotor current;
- K_{ξ} coil factor of rotor (for squirrelcage motor is 1);
- ξ degree of rotor harmonics;
- w_r angular speed of rotor.

Degree of stator harmonics is formulated by

$$\nu = p(6c_1 \pm 1) \quad (10)$$

Degree of rotor harmonics is formulated by

$$\xi = \pm \nu + c_2 \frac{Z_{rt}}{p} \quad (11)$$

$$c_2 = 0, 1, 2, 3, \dots$$

In calculation of airgap flux density we only use mmf of stator.

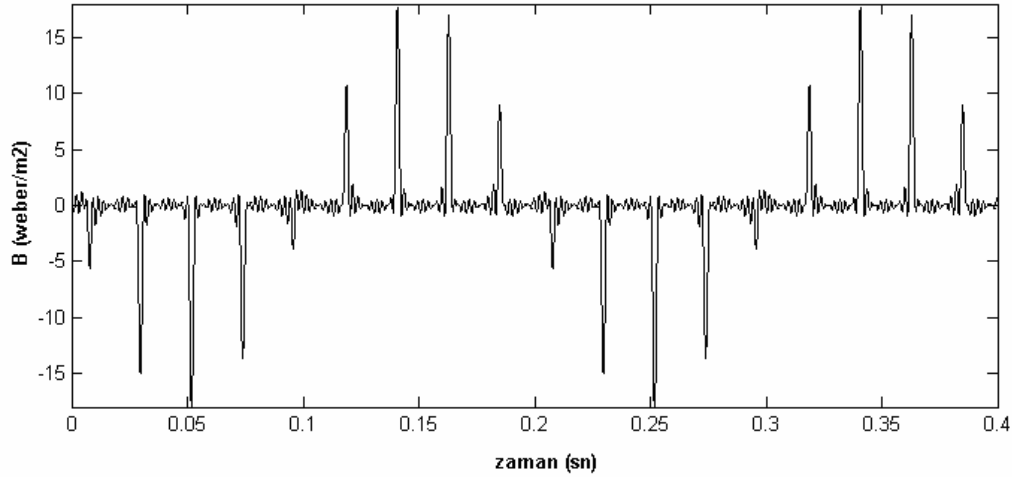


Fig. 6 variation of magnetic flux density in dynamic eccentricity situation.

Rotor mmf can be used to improve this study.

Permeance is calculated as following equation,

$$\lambda = \lambda_{\text{slot}} \cdot \lambda_{\text{saturation}} \cdot \lambda_{\text{d_eccentricity}} \cdot \lambda_{\text{s_eccentricity}} \quad (12)$$

Slot and saturation effects are not included in calculation of permeance. After assumptions, permeance can be written as air-gap variation due to eccentricity.

$$\lambda \approx \frac{1}{\delta(\theta)} \quad (13)$$

This formula is rearranged according to static eccentricity. Permeance of static eccentricity can be defined as

$$\lambda = \frac{1}{\delta(\theta)} = \frac{1}{\delta - a \cdot \cos(\theta)} = \frac{1}{\delta(1 - \varepsilon \cdot \cos(\theta))} \quad (14)$$

a is displacement of rotor. ε is relative displacement of rotor that is given by

$$\varepsilon = \frac{a}{\delta} \quad (15)$$

Fourier series is applied to permeance of static eccentricity. Result of fourier analysis is

$$\lambda_{\text{se}} = \frac{1}{\delta} \cdot (\lambda_0 + \lambda_1 \cdot \cos(\theta) + \lambda_2 \cdot \cos(2\theta) + \dots) \quad (16)$$

where

$$\lambda_0 = \frac{1}{\sqrt{1 - \varepsilon^2}} \quad (17)$$

and

$$\lambda_i = 2 \cdot \frac{(1 - \sqrt{1 - \varepsilon^2})^i}{\varepsilon^i \cdot \sqrt{1 - \varepsilon^2}} \quad i=1,2,3,\dots \quad (18)$$

By using (8),(10),(13)-(18) in (7), magnetic flux density is calculated. Fourier analysis of magnetic flux density shows frequencies of static eccentricity on current signal.

Permeance for dynamic eccentricity is same with static eccentricity, but only it rotates with rotor. (16) can be rearranged for dynamic eccentricity.

$$\lambda_{\text{de}} = \frac{1}{\delta} (\lambda_0 + \lambda_1 \cdot \cos(\theta - w_r \cdot t) + \lambda_2 \cdot \cos(2 \cdot (\theta - w_r \cdot t)) + \dots) \quad (19)$$

According to appendix table, magnetic flux density in dynamic eccentricity is given in Fig. 6 and frequency analysis of magnetic flux density in Fig. 7.

D. Formula of Thomson

In reference [10], eccentricity related frequencies are predicted by

$$f_{\text{st_current}} = f \left\{ \pm \tau_{\text{de}} \cdot \frac{(1-s)}{p} \pm \tau_{\text{st_mmf}} \right\} \quad (20)$$

where

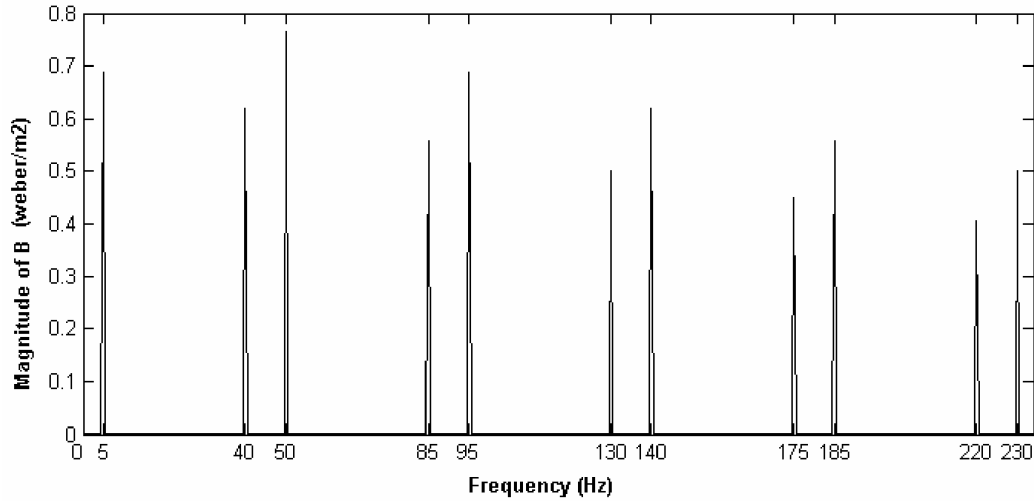


Fig. 7 frequency spectrum of magnetic flux density in dynamic eccentricity situation.

s slip;

f electrical supply frequency;

$\tau_{de} = 1, 2, 3, \dots$;

$\tau_{st_mmf} = 1$ effect of stator mmf.

Value of τ_{st_mmf} takes only 1, because the number in front of w in (4) equals to 1. Value of τ_{st_mmf} ranges from $-\infty$ to $+\infty$ in reference [10]. In reference [11], it is represented by $\pm 1, \pm 3, \pm 5, \pm 7 \dots$ values. In both of them, value of τ_{st_mmf} is wrong.

In reference [6]-[8], this value is used as 1 to monitor the behavior of the sidebands around the fundamental frequency safely. Nonetheless, τ_{st_mmf} can not take other values.

III. BEARING DAMAGE

A. Bearing Faults and Effect on Vibration Signal

There are four parts in bearing, cage, balls, inner and outer rings. These parts can be damaged due to over load, corrosion, improper lubrication and installation. Over load or weak lubrication causes friction. As a result of friction, temperature increases, so that oil lost its properties. Also, water and acid is dangerous for oil. Another point for damage, current flows on bearings, because of voltage difference between stator and rotor. Oil behaves as a dielectric material in condenser. These faults produce small particles in bearing.

Each damaged part on bearing leads to vibration at specific frequencies. In the case of a bearing damage on inner and outer ring, characteristic frequencies are respectively identified as follows

$$f_{inner} = \frac{Z_b}{2} \cdot f_r \cdot \left(1 + 2 \cdot \left(\frac{d_w \cdot \cos(\alpha)}{d_1 + d_2} \right) \right) \quad (21)$$

$$f_{outer} = \frac{Z_b}{2} \cdot f_r \cdot \left(1 - 2 \cdot \left(\frac{d_w \cdot \cos(\alpha)}{d_1 + d_2} \right) \right) \quad (22)$$

where

- Z_b number of balls;
- f_r frequency of rotor rotation;
- d_w diameter of ball;
- d_1 diameter of inner ring;
- d_2 diameter of outer ring;
- α contact angle of balls.

In reference [16], a real time measurement setup compares different methods to detect the bearing fault.

B. Bearing Damage Effect on Current Signal

Reference [17] defines formula to calculate the frequencies on current signal because of bearing faults.

$$f_{current} = |f \pm k \cdot f_k| \quad (23)$$

f_k is one of the characteristic vibration frequency of bearing faults, $k = 1, 2, 3, \dots$

Bearing faults should be considered as a sudden eccentricity problem in order to accurately predict the results of bearing faults. It is known that bearing faults induce vibration at characteristic frequencies. As a result of vibration,

displacement of rotor shaft appears. Thus, air-gap changes according to vibration.

If outer ring damage occurs, it would be described as a sudden static eccentricity. Since, outer ring do not rotate with rotor, the static eccentricity equals to outer ring damage as in Fig. 8.

Inner ring damage is different than outer ring damage, because inner ring rotates with rotor. Therefore, it is assumed as a sudden dynamic eccentricity as in Fig. 9.

Refer to (21) and (22), characteristic frequencies are evaluated for inner and outer rings, respectively 243 Hz and 162 Hz. According to (23), inner ring damage related current frequencies are 293 Hz and 193 Hz for $k=1$. Outer ring damage current frequencies are 212 Hz and 112 Hz for $k=1$, 374 Hz and 274 Hz for $k=2$, and 536 Hz and 436 Hz for $k=3$.

Results of computer program are shown in Fig. 10 and Fig. 11. Formula of Schoen is verified by computer program. Also, at Fig. 10 for inner ring damage, additional frequencies appear. These frequencies are based on formula of Thomson. Refer to (20), some of the values are 220 Hz, 265 Hz and 275 Hz. This means, every frequency in Thomson's formula for current signal do not only describe eccentricity, but also describe bearing faults. It should be answered that what is the difference between eccentricity and bearing fault.

We can not recognize the fault exactly by using current signature analysis, but reference [4] emphasizes that current signature analysis is sufficient to detect eccentricity and bearing faults.

Another point, magnitude of dynamic eccentricity related frequencies in Fig. 7 are bigger than inner ring damaged related frequencies in Fig. 10. The reason is that one point damaged bearing is simulated. Magnitude of the frequencies shows the severity of defect on bearing.

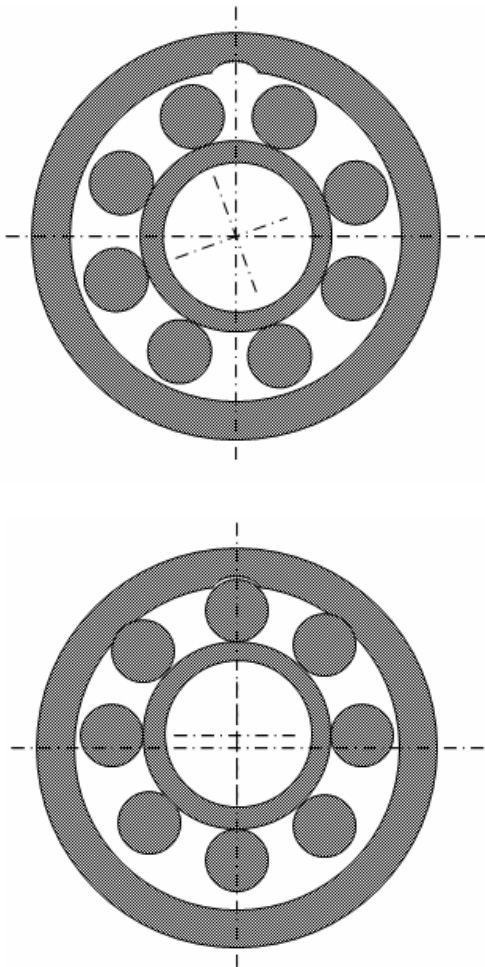


Fig. 8 animation of outer ring damage

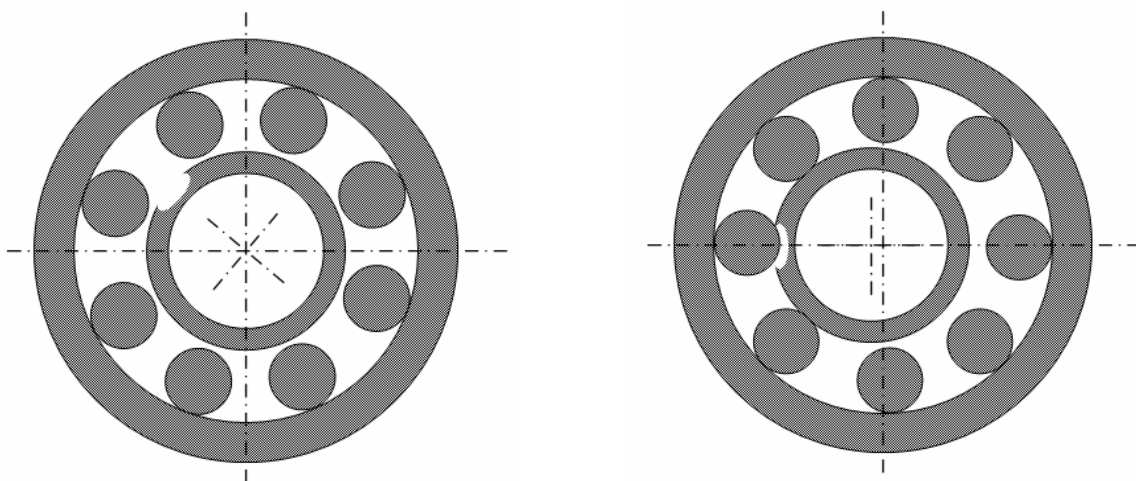


Fig. 9 animation of inner ring damage

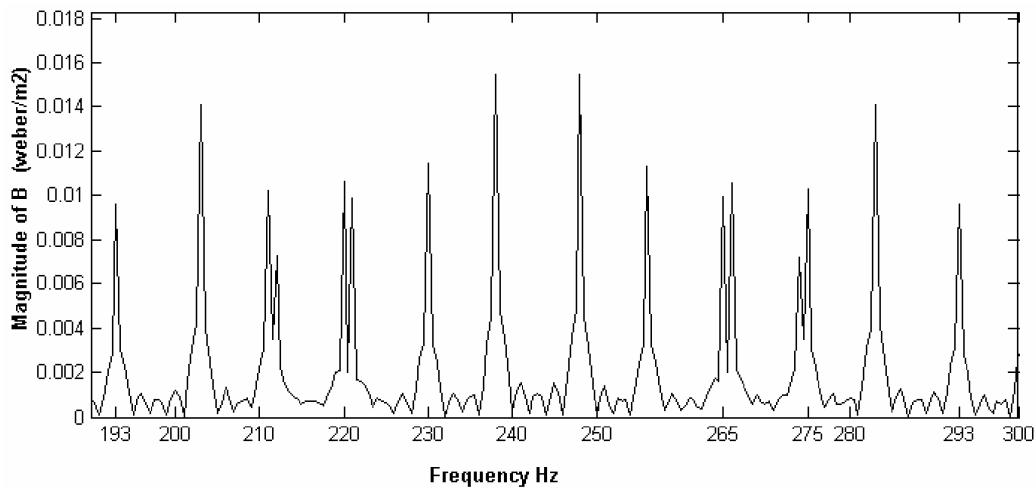


Fig. 10 frequency spectrum of magnetic flux density when inner ring is damaged

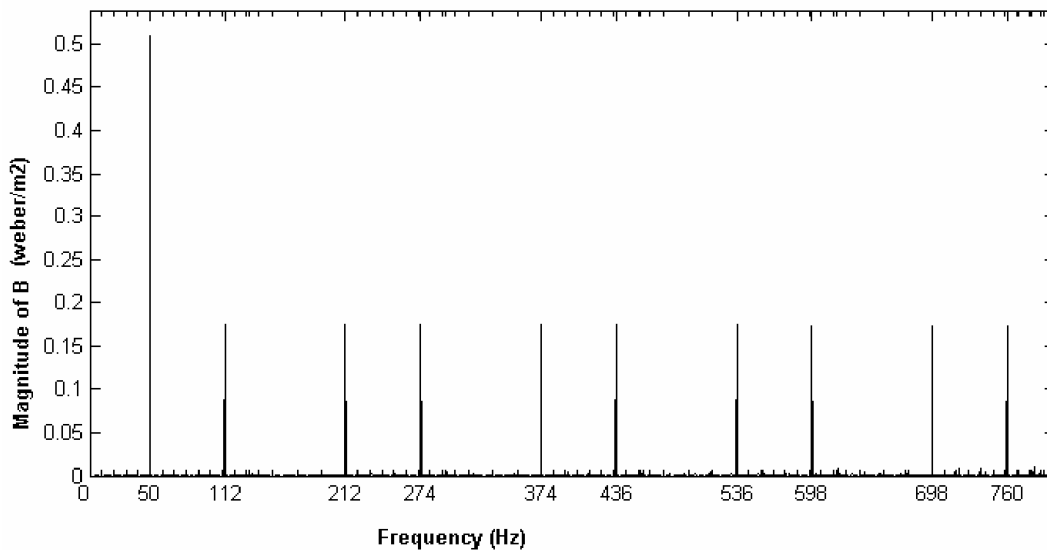


Fig. 11 frequency spectrum of magnetic flux density when outer ring is damaged

IV. CONCLUSION

τ_{st_mmf} equals to 1. Thomson and Vas have used different values. Use of other τ_{st_mmf} values result with wrong fault decision.

If eccentricity related frequencies are detected in current signal. Bearing damage effect should be searched. Vibration measurement is enough for bearing damage detection.

Both of the results are critical to find faults. The reliability of Neural Networks for fault detection can be improved by using current and vibration signals to differentiate the bearing damage and eccentricity.

APPENDIX

$d_w=12$ mm, $d_1=80$ mm, $d_2=40$ mm, $f_r=45$ Hz, $Z_b=9$,
 $\alpha=0$ rad, $f=50$ Hz, $s=0.1$, $p=1$, $\epsilon=0.9$, $\delta=2$ mm,
 $I_{st}=5A$ (rms), $N=200$, $K_v=1$, $\mu=4\pi \cdot 10^{-7}$ H/m.

REFERENCES

- [1] S. Nandi, H. A. Toliyat, and X. Li, "Condition monitoring and fault diagnosis of electrical motors-a review," *IEEE Trans. Energy Convers.*, vol. 20, no. 5, pp. 719–728, Dec. 2005.
- [2] M. E. H. Benbouzid, "A review of induction motors signature analysis as a medium for faults detection," *IEEE Trans. Indus. Elec.*, vol. 47, no. 5, pp. 984–993, Oct. 2000.
- [3] A. Siddique, G. S. Yadava, and B. Singh, "A review of stator fault monitoring techniques of induction motors," *IEEE Trans. Energy Convers.*, vol. 20, no. 1, pp. 106–113, March 2005.
- [4] N. Mehla, and R. Dahiya, "An approach of condition monitoring of induction motor using mcsa," *International Journal of Systems*

Applications, Engineering & Development, vol. 1, issue 1, pp. 13–17, July 2007.

- [5] N. Mehla, and R. Dahiya, “Motor current signature analysis and its applications in induction motor fault diagnosis” *International Journal of Systems Applications, Engineering & Development*, vol. 2, issue 1, pp. 29–35, August 2007.
- [6] A. Nasiri, and M. Hosseini, “Fuzzy-wavelet for detection of eccentricity in induction motors,” *4th WSEAS Int. Con. on Power Engineering Systems, ICOPES'05*, Rio de Janeiro, Brazil, April 2005.
- [7] E. L. Bonaldii, L. E. Borges, G. Lambert, and L. E. L. Oliveira “A rough sets based classifier for induction motors fault diagnosis,” *WSEAS Trans. on Systems*, vol. 2, issue 2, pp. 2271-2278, April 2003.
- [8] N. Hu, Y. Zhang, F. Gu, G. Qin, and A. Ball, “Early fault detection using a novel spectrum enhancement method for motor current signature analysis,” *7th WSEAS Int. Con. on Artificial Intelligence, Knowledge Engineering and Data Bases, AIKED'08*, University of Cambridge, UK, February 2008.
- [9] V. Kontargyri, C. Tsirekis, S. Kabanaros, A. Sakarellos, A. Moronis, and N. Kolliopoulos, “An expert system for fault diagnosis, repairing and maintenance of electric machines,” *6th WSEAS Int. Con. on Electrical Engineering*, Istanbul, Turkey, May 2007.
- [10] J. R. Cameron, W. T. Thomson, and A. B. Dow, “Vibration and current monitoring for detecting airgap eccentricity in large induction motors,” *IEE Proc. Inst. Elect. Eng. B*, vol. 133, no. 3, pp. 155–163, May 1986.
- [11] P. Vas, *Parameter Estimation, Condition Monitoring, and Diagnosis of Electrical Machines*. Oxford, U.K.: Clarendon, 1993, pp. 307–308.
- [12] H. Guldemir, “Detection of airgap eccentricity using line current spectrum of induction motors,” *Elsevier Science Electric Power Systems Research.*, 64, no. 2, pp. 109–117, Dec. 2003.
- [13] D. K. Cheng, *Field and Wave Electromagnetics*. New York: Addison-Wesley Company, 1989.
- [14] P. L. Alger, *Induction Machines Their Behavior and Uses*. Switzerland: Gordon and Breach Science Publishers SA, 1970.
- [15] B. Heller, and V. Hamata, *Harmonic Field Effects in Induction Machines*. New York: Elsevier, 1977.
- [16] A. Fernandez, J. Bilbao, I. Bediaga, A. Gaston, and J. Hernandez, “Feasibility study on diagnostic methods for detection of bearing faults at an early stage,” *WSEAS Int. Con. on Dynamic Systems and Control*, pp. 113-118, Venice, Italy, November 2005.
- [17] R. R. Schoen, T. G. Habetler, F. Kamran and R. G. Bartheld, “Motor bearing damage detection using stator current monitoring,” *IEEE Trans. Indus. Appl.*, vol. 31, no. 6, pp. 1274–1279, Nov./Dec. 1995.
- [18] S. J. Yang, *Low-noise electrical motors*. Oxford, New York: Clarendon Press, 1981, pp. 15–36.
- [19] I. Boldea and S. A. Nasar, *The Induction Machine Handbook*. New York: CRC Press, 2002, ch. 10.
- [20] Eschmann, Hasbargen and Weigand, *Ball and Roller Bearings Theory, Design, and Application*. New York: John Wiley & Sons Ltd., 1985, pp. 78–95.



Ilker Ozelgin was born in Bursa, Turkey in 1981. He received the B.S. degrees in mechanical engineering and electrical engineering in 2004 and 2005 respectively, and the M.S. degree in control and automation engineering program in 2006 from Istanbul Technical University, Istanbul, Turkey.

His research interests include fault detection of electrical machines, modeling of vehicles and electric machines, microcontrollers and hybrid electric vehicles. He works about hybrid electric vehicles in Ford-Otosan, Kocaeli, Turkey.